IEEE Access
Multidisciplinary : Rapid Review : Open Access Journal

Received 29 August 2022, accepted 5 September 2022, date of publication 14 September 2022, date of current version 22 September 2022.

Digital Object Identifier 10.1109/ACCESS.2022.3206022

RESEARCH ARTICLE

Design of a Memristor-Based 2-DOF PI Controller and Testing of Its Temperature Profile Tracking in a Heat Flow System

KAMIL ORMAN
Department of Computer Engineering, Erzincan Binali Yıldırım University, 24100 Erzincan, Turkey
e-mail: korman@erzincan.edu.tr

ABSTRACT In this study, a memristor-based 2-DOF PI controller (2-DOF Mem-PI) was designed for the temperature profile tracking control of a model of heat flow experiment (HFE) setup. A simulation study is presented in which the performance of the designed controller is compared with a standard 2-DOF PI controller. Compared to 1-DOF control structures, 2-DOF controllers that include an extra adjustable parameter perform better in terms of response to disturbances and improving the transient response of the system. In addition, memristor-based controllers (Mem-PI and 2-DOF Mem-PI) and standard controllers (PI and 2-DOF PI) were compared and it was determined that because of the variable memristance value, the control structures containing memristors showed an adaptive feature. The simulation results demonstrated the success of the proposed controller in temperature profile reference tracking and showed the memristor to be applicable in nonlinear control structures.

INDEX TERMS 2-DOF PI controller, memristor, memristor-based controller, temperature profile control.

I. INTRODUCTION

Temperature and temperature control are important factors in different classes and processes of industrial production that should be taken into consideration, especially in terms of the safety of the production facility and product quality [1]. In practice, tracking the reference temperature profile, keeping the temperature at a set point, and controlling the distribution of the atmospheric temperature are the most common temperature control tasks encountered. Temperature reference tracking control is also important, as it requires flexible, stable, and adaptable control because of various control theory issues such as the operating environment, varying time constants, and disturbing external factors that can be seen in real systems. Ahn *et al.* introduced a new analytical tuning method for the fractional-order integral derivative (FO-ID) $I\alpha D\beta$ controller and applied it to analyze the heat flow in the obtained controller heat flow experiment (HFE) module. In addition, they presented comprehensive simulation results to demonstrate the practical and simple nature of the proposed new tuning rules [2]. Al-Saggaf *et al.* proposed a new model-based analytical design for fractional-order controllers. The efficiency and performance of this proposed method was demonstrated by simulations and on a heat flow platform experimentally [3]. In another study, a control design approach for input saturated linear systems was presented. Two practical applications in both a heat flow system and a liquid flow system were presented to verify the effectiveness of the proposed control design method. The effectiveness of the proposed approach was demonstrated by experimental results [4]. Hernandez-Perez *et al.* investigated the stabilization problem of the class of highly unstable time-delayed systems. In the control structure they proposed, a new control law called the PIf controller, consisting of a standard PI controller and a first-order low-pass filter, was used. The performance of the proposed controller was tested in a thermal flow assembly equipped with a time delay and a recycling path, and it was reported that an adequate performance had been achieved [5]. In order to obtain a generally acceptable process response, Nath *et al.* proposed

The associate editor coordinating the review of this manuscript and approving it for publication was Qi Zhou.

an automatic tuning scheme for the traditional internal model control - PID (IMC-PID) controller by changing the single setting parameter depending on the latest process operating conditions [6]. They also demonstrated the superiority of the proposed fuzzy rule-based automatic adjustment scheme with the results of real-time experiments on level and temperature control processes.

The proportional-integral / proportional-integral-derivative (PI/PID) controller structure is a control mechanism that has a wide range of uses such as in electronic devices, mechanical devices, and pneumatic systems, and for process control in different fields of industry [7], [8], [9], [10]. In addition, the advantages of the two-degree-of-freedom (2-DOF) control structure over the one-degree-of-freedom (1-DOF) control structure were stated by Horowitz [11]. The 2-DOF controller structure was developed for situations where a 1-DOF controller structure is insufficient. By adding the β parameter to the controller structure, better performance is provided in terms of maintaining the response of the controller to disturbances and improving the transient response of the system. In recent years, there have been many studies based on different tuning and optimization algorithms proposed for 2-DOF control structures [12], [13], [14], [15], [16].

The memristor was first described by L.Chua in 1971 as a memory resistor and was produced by HP researchers in 2008 [17], [18]. The physically realized memristor quickly managed to attract the attention of researchers, but its application as a discrete circuit element has been delayed. However, researchers have realized many models and circuits by working on circuits that act as memristors [19], [20], [21], [22], [23], [24]. Recently, testing of the memristor has begun in the control field, and memristor-based controllers have been suggested by researchers [25], [26], [27], [28], [29], [30], [31], [32]. In applications such as variable gain and automatic gain control, the TiO_2 memristor model was used as the memristor model due to the simplified expressions and the same ideal physical behavior [33], [34], [35]. In particular, once controllers designed using memristor emulator circuits increase and production has begun, their use will be possible in the future.

In previous studies, unlike this study, 1-dof PI controller with memristor-based integrator circuit was designed and applied to the heat flow system [28]. In [30], a PD control structure was obtained with a memristor derivative circuit and applied to the ball and beam system. In [31], a sliding mode control approach was obtained by using a memristor-based derivative circuit and simulation results for speed control of BLDC motor were presented.

In this study, a novel memristor-based 2-DOF PI controller structure was proposed and a comparison was made between standard PI, standard 2-DOF PI, 1-DOF mem-PI and 2-DOF mem-PI controllers. The simulation model of Quanser's heat flow experimental (HFE) setup was used to test the temperature profile tracking performance of the proposed controller and simulation results were presented.

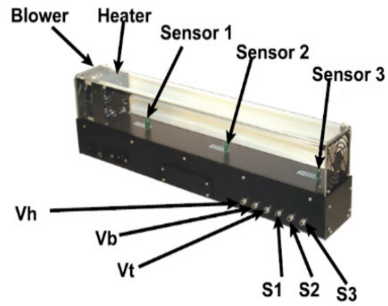

FIGURE 1. Heat flow experimental (HFE) setup https://www.quanser.com/products/heat-flow-experiment/.

II. HEAT FLOW EXPERIMENTAL (HFE) SETUP

The heat flow experimental (HFE) setup produced by Quanser, which enables simulation and experimental studies related to the control of a heat flow system, is shown in Figure 1. The air mass heated by the coil is transported through a channel with three temperature sensors at fixed distances using a fan whose speed can be measured.

Although it is difficult to obtain a thermodynamic model of the system, the state variables of this system can be determined as follows:

$$\frac{d}{dt}T_n = F(V_h, V_b, T_a, x_n) \tag{1}$$

where V_h and V_b are the blower and heater voltages, respectively. Similarly, T_n and T_a are the n^{th} sensor and ambient temperature, respectively, and x_n indicates the distance between the heater and the n^{th} sensor.

The first-order transfer function model of the system, as follows, is sufficient to design a temperature controller.

$$T_n(s) = \frac{K_n V_h(s)}{\tau_n s + 1} \tag{2}$$

where τ_n and K_n are the time constant and steady state gain for the n^{th} sensor, respectively. The voltage-to-temperature transfer function of the HFE system is as follows [36]:

$$G(s) = \frac{T(s)}{V(s)} = \frac{K}{\tau s + 1} \tag{3}$$

In practical applications, time delay and dead time occurs in real systems [37], [38]. In the handbook presented by Quanser, dead time is not included as in the equation given in (3).

III. MEMRISTORS

In 1971, Leon Chua claimed that there should be a fourth basic circuit element in addition to the resistor, inductor, and capacitor. He stated that it is a power-consuming element such as a resistor, that it cannot be modeled by other circuit elements, and that its value can be expressed by the ratio of voltage to current depending on the load [17]. The memristor, which was always thought of as a mathematical concept, was produced by an HP research team about 36 years later [18].

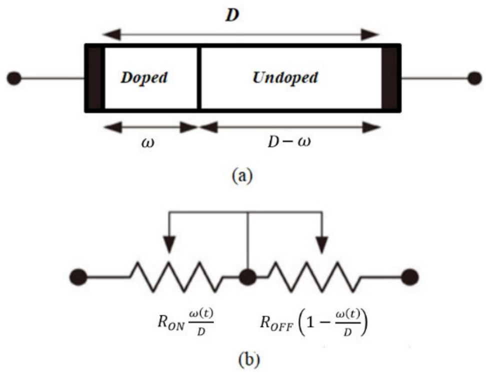

FIGURE 2. a) Physical structure of a memristor with total body length D, and doped and undoped region lengths ω and D-ω respectively; b) Two-resistor model of the memristor.

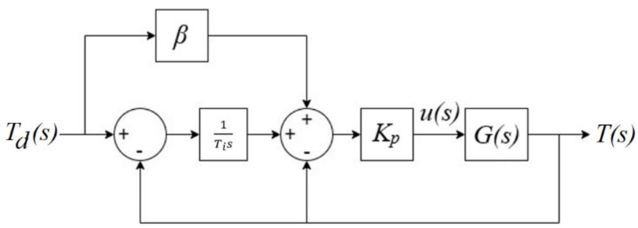

FIGURE 3. Block diagram of 2-DOF PI-based temperature control for HFE.

The relationship between voltage and current recommended by the HP research group for a TiO_2 memristor [18] is:

$$V\ (t) = Mi\ (t) = \left[R_{ON} \frac{\omega\ (t)}{D} + R_{OFF} \left(1 - \frac{\omega\ (t)}{D} \right) \right] i(t) \tag{4}$$

where ω is the state variable of the device, M represents the memristance, R_{ON} indicates low resistance states, R_{OFF} indicates high resistance states, and D represent the total length of the TiO_2 memristor, respectively.

The memristance value, which is directly dependent on the change of the ω value, is defined as:

$$\frac{d\omega\ (t)}{dt} = \mu_v \frac{R_{ON}}{D} i\ (t) \tag{5}$$

Here, μ_v is the mobility of the memristor [18]. The physical structure of the memristor is given in Figure 2.

IV. CONTROLLER DESIGN

A. 2-DOF PI CONTROLLER

Using the temperature profile tracking error based on the current temperature T and the desired temperature value T_d, an error signal can be defined for the controller design as follows:

$$e\ (t) = T_d\ (t) - T\ (t) \tag{6}$$

The block diagram of the 2-DOF PI-based closed-loop control function for temperature profile tracking in the HFE simulation model is given in Figure 3.

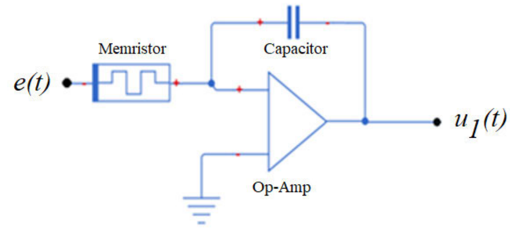

FIGURE 4. Memristor-based integrator circuit.

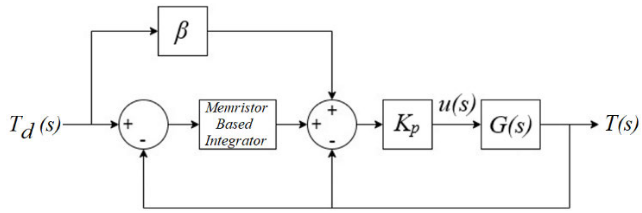

FIGURE 5. Block diagram of the 2-DOF PI controllers based on a memristor for temperature profile tracking.

The control signal *u(s)* indicated in the block diagram in Figure 3 can be expressed as follows:

$$u\ (s) = K_p \left[\beta T_d\ (s) + \frac{1}{T_i s} (T_d\ (s) - T\ (s)) - T(s) \right] \tag{7}$$

If this equation is rearranged,

$$u\ (s) = K_p \left[\{\beta T_d\ (s) - T(s)\} + \frac{1}{T_i s} \{T_d\ (s) - T\ (s)\} \right] \tag{8}$$

$$u\ (s) = K_p \left[\{\beta T_d\ (s) - T(s)\} + \frac{1}{T_i s} \{e\ (s)\} \right] \tag{9}$$

is obtained, where *e(s)* is the error signal specified in (6).

B. MEMRISTOR-BASED INTEGRATOR

In the integrator circuit shown in Figure 4, the resistance of the memristor is automatically changed with the voltage applied to it, so that an adjustable gain can be obtained [39].

The mathematical expression of the memristor-based integrator circuit can be written as follows:

$$u_1\ (t) = \frac{1}{MC} \int_0^t e\ (\tau)\ d\tau \tag{10}$$

where C is capacitance and M represents the memristance.

C. MEMRISTOR-BASED 2-DOF PI CONTROLLER

If the integration process in the 2-DOF PI control structure given in Figure 3 is carried out with the memristor-based integrator circuit given in Figure 4, a memristor-based 2-DOF PI controller structure is obtained. A block diagram of the temperature profile tracking control of the HFE with the memristor-based 2-DOF PI (2-DOF Mem-PI) approach is given in Figure 5.

Using (4), (6), (9) and (10), the control signal *u(s)* in the proposed control structure can be written as follows:

$$u\ (s) = K_p \left[\{\beta T_d\ (s) - T(s)\} + \frac{1}{MCs} \{e\ (s)\} \right] \tag{11}$$

$$u(s) = K_p \left[\{\beta T_d(s) - T(s)\} + \frac{1}{\left[R_{ON}\frac{x(t)}{D} + R_{OFF}\left(1 - \frac{x(t)}{D}\right)\right] Cs} \times \{T_d(s) - T(s)\} \right] \quad (12)$$

D. DETERMINATION OF CONTROLLER PARAMETERS

Parameters in the proposed control structure were determined using the multiple dominant pole method (MDPM) as in the study presented by Viteckova and Vitecek [40]. The definition of the HFE as a first-order plus time-delay (FOPTD) plant in the Quanser instruction manual is as follows [36]:

$$\frac{Y(s)}{U(s)} = \frac{K}{\tau s + 1} \quad (13)$$

By solving the system of equations given in (14), adjustable controller parameters and multiple dominant poles $\hat{s}_{p+1}$ can be obtained. The FOPTD system and the quasi-polynomial characteristic of the standard PI controller described in [38] are given in (15) and (16), respectively.

$$\frac{d^j N(s)}{ds^j} = 0 \quad \text{for } j = 0, 1, \ldots p \quad (14)$$

$$G(s) = \frac{K}{Ts + 1} e^{-Ls} \quad (15)$$

$$N(s) = \left(Ts^2 + s\right) e^{Ls} + KK_p \left(s + \frac{1}{T_I}\right) \quad (16)$$

where p is the number of adjustable controller parameters, K is plant gain, L is time delay, K_P is controller gain, T_I is integral time, and $N(s)$ is the quasipolynomial characteristic of the control system. The form of the standard PI controller adjusted with MDPM and the approximate control system transfer functions to be designed for a plant expressed as in (16) is given in (17) [40].

$$C(s) = \frac{\hat{T}_I s + 1}{\left(\frac{1}{|\hat{s}_3|} s + 1\right)^3} e^{-Ls} \quad (17)$$

In Table-1 presented in [40], in light of (15) and (17), it is stated that for p = 2, two adjustable controller parameters $\hat{K}_p$ and $\hat{T}_I$ and triple dominant pole $\hat{s}_3$ values can be obtained as indicated below:

$$\hat{s}_3 = -\frac{2}{L} - \frac{1}{LT} + \sqrt{\frac{2}{L^2} + \frac{1}{4T^2}} \quad (18)$$

$$\hat{K}_p = -\frac{1}{K}\left[LT\hat{s}_3^2 + (2T + L)\hat{s}_3 + 1\right] e^{L\hat{s}_3} \quad (19)$$

$$\hat{T}_I = -\frac{LT\hat{s}_3^2 + (2T + L)\hat{s}_3 + 1}{(LT\hat{s}_3 + T + L)\hat{s}_3^2} \quad (20)$$

$$\hat{\beta} = min\left\{\frac{1}{\hat{T}_I |\hat{s}_3|}, 1\right\} \quad (21)$$

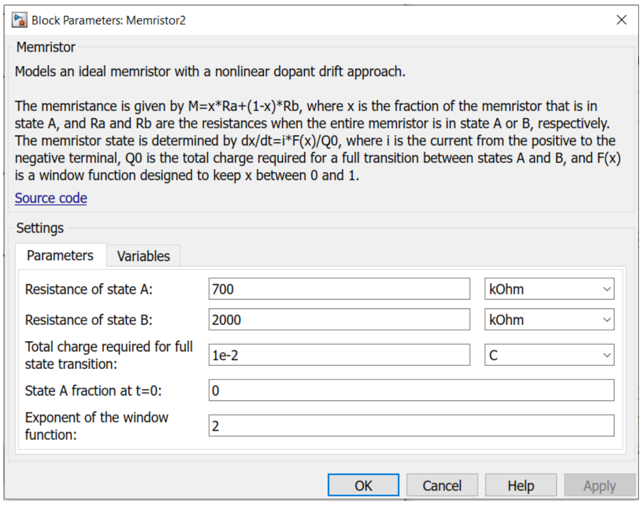

FIGURE 6. Memristor parameters in MATLAB/Simulink. (https://www.mathworks.com/help/physmod/simscape/ref/memristor.html).

In the Quanser instruction manual, the values determined for the step response were K = 10, T = 5 s and L = 1 [36]. Considering these values, if (18), (19), (20), and (21) are solved, the parameters of the 2-DOF PI controller given in (8) are obtained:

$$\hat{s}_3 = -0.6823 \quad \hat{K}_p = 0.2112$$
$$\hat{T}_I = 3.4668 \quad \hat{\beta} = 0.4228$$

V. SIMULATION

In this study, the memristor model in the MATLAB (2016a)/Simulink Simscape model library was used. The R_{ON} and R_{OFF} resistance values in (4) are used as state-A and state-B resistors in the model parameter given in Figure 6. Considering the memristor model parameters and (10), it was determined that $MC = T_I = \hat{T}_I$ and hence, $C = 1.7334\ \mu F$. The designed 2-DOF mem-PI controllers and the standard 2-DOF PI controllers were compared in terms of temperature profile tracking performance and the results are given in Figures 7-12. The reference temperature profile signal includes sudden and smooth changes.

In Figure 7, both controllers are seen to perform similarly in terms of time to reach the reference. However, the 2-DOF Mem-PI controller was more successful than the 2-DOF PI controller in terms of eliminating the error early on.

Figure 8 gives the control signals of the 2-DOF Mem-PI controller and the 2-DOF PI controller. Both control signals have a similar form, but the 2-DOF Mem-PI control signal is smoother than that of the 2-DOF PI.

Considering the previous study of [28], it was thought to examine the relationship between memristor-based controllers and classical controllers, and for this purpose, the temperature control of HFE for the same reference signal was tested with the standard 1-DOF PI, 1-DOF Mem-PI, standard 2-DOF PI, and 2-DOF Mem-PI controllers. The reference temperature profile tracking simulation results of these four controllers are given in Figure 9.

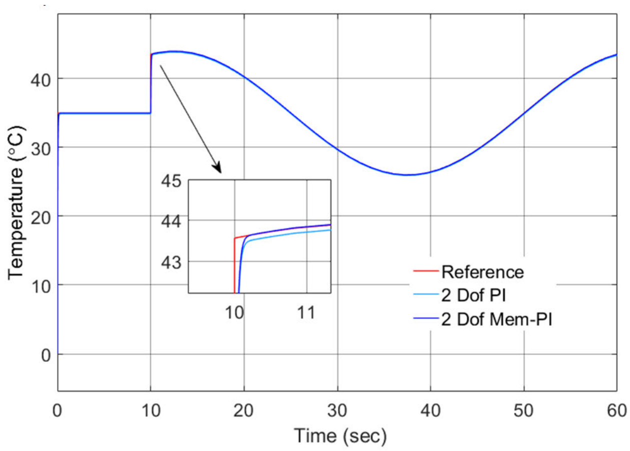

FIGURE 7. Simulation result of temperature profile tracking control of the HFE using 2-DOF PI and 2-DOF Mem-PI controllers.

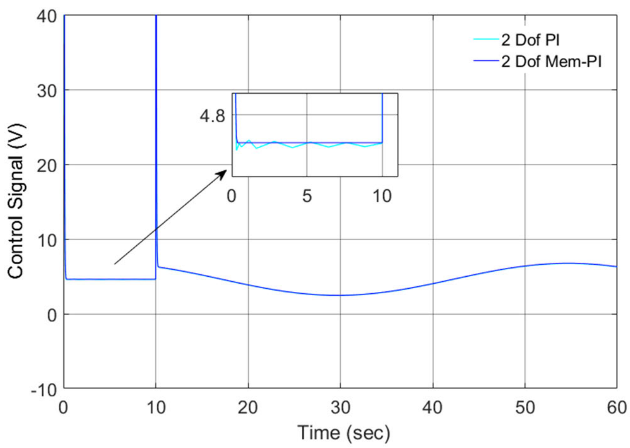

FIGURE 8. Control signals of 2-DOF PI and 2-DOF Mem-PI controllers.

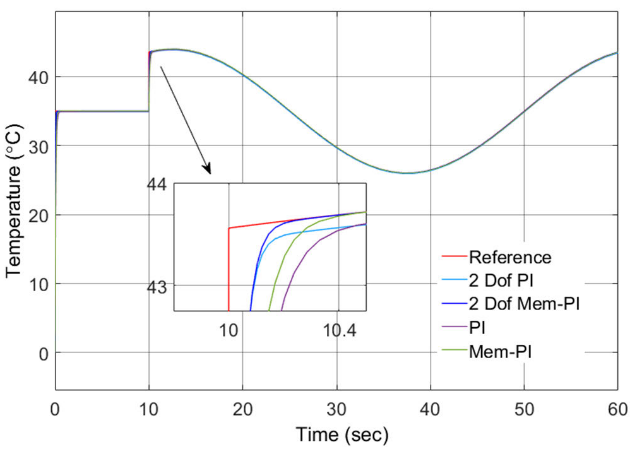

FIGURE 9. Simulation result of temperature profile tracking control of the HFE using Standard PI, Mem-PI, 2-DOF PI and 2-DOF Mem-PI controllers.

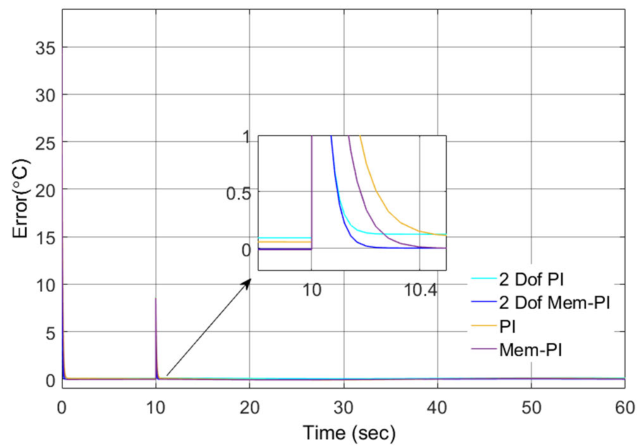

FIGURE 10. Error signals of Standard PI, Mem-PI, 2-DOF PI and 2-DOF Mem-PI.

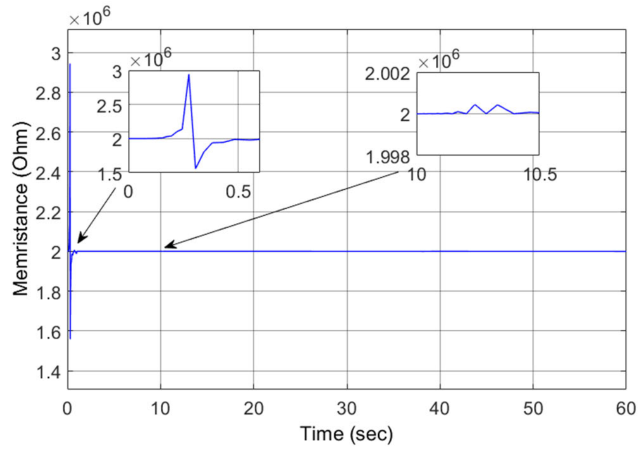

FIGURE 11. Memristance value of the memristor.

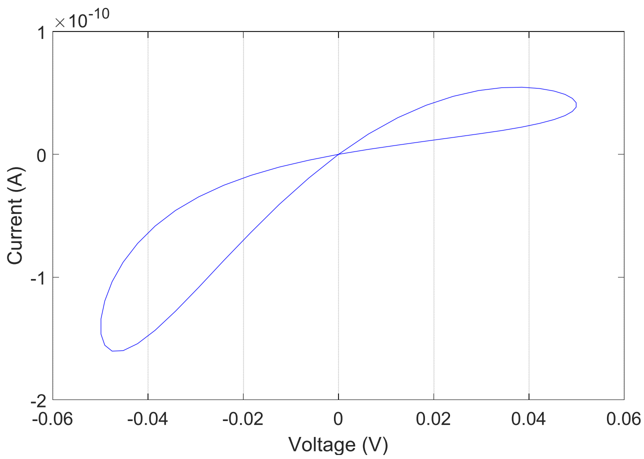

FIGURE 12. The memristor current-voltage relationship.

The graphic in Figure 9 shows that, regardless of whether the controller was standard or memristor-based, the 2-DOF control structures reached the reference earlier than the 1-DOF control structures. On the other hand, the memristor-based control structures (Mem-PI and 2-DOF Mem-PI) eliminated the error more quickly than the standard control structures (PI and 2-DOF PI). This is more clearly seen where the error signals are given in Figure 10.

Figure 11 gives the simulation results of the change of the memristance (M) value under the adjusted parameter values of the memristor used in the simulation study. During sudden changes in the reference, the memristance value is also seen to change, thus realizing an adaptation function.

Memristors exhibit a hysteresis voltage-current relationship when a sinusoidal signal is applied, and the voltage-current relationship of the memristor model used in this study is given in Figure 12.

VI. DISCUSSIONS AND CONCLUSION

In practice, many control systems have a time delay within the closed loop of the system, which affects the stability of the system. The time delay for the heat flow system given in (15) was represented by e^{-Ls}. where L is the time delay. One of the valid methods used to determine the effect of time delay on the relative stability of the feedback system is the Nyquist criterion. The Nyquist criterion remains valid for a time-delayed system, as the factor e^{-Ls}, which adds a phase shift to the frequency response without changing the magnitude curve, does not introduce any additional poles or zeros in the contour. Also, a time delay e^{-Ls} introduces an additional phase delay in the feedback system and makes the system less stable. In the stability analysis of such systems, most analytical tools are considered and the transfer functions of the systems are defined by rational functions or a finite set of ordinary constant coefficient differential equations. The Padé approximation can be used to obtain a rational function approximation of the time delay. The Padé approximation uses a series expansion of the transcendental function e^{-Ls} and matches as many coefficients as possible with a series expansion of a rational function of specified order. In practical applications of heat flow systems, time delay occurs. However, dead time and time delay are ignored in the model used in this study. In addition, stability analysis of the proposed controller was not performed.

In this study, 2-DOF PI controllers based on memristors were tested via HFE temperature profile tracking control and simulation results were presented. It was demonstrated that the memristor, known as the missing circuit element, can be applied in 2-DOF control structures. Results of this simulation study showed that the 2-DOF Mem-PI controller was successful in the temperature profile tracking control of the HFE. When Figure 9 was examined, it was observed that no overshoot occurred in all the compared controllers. Additionally, the 2-DOF control structures were faster in terms of reaching the reference compared to the 1-DOF control structures because of the extra adjustable parameter. As can be seen in Figure 9, 2-DOF control structures reached the reference approximately 1 second earlier than 1-DOF control structures. On the other hand, because they contained an extra parameter, the 2-DOF control structures were faster in eliminating error compared to the 1-DOF control structures. Figure 10 shows that the error elimination time of the 2-DOF PI controller is approximately 46% lower than the 1-DOF PI controller. Furthermore, the Mem-PI and 2-DOF Mem-PI controllers designed using a memristor were successful in eliminating error faster than the PI and 2-DOF PI standard controllers because of their variable memristance value. Depending on the voltage change of the error signal at the controller input, the resistance value of the memristor takes a value between the R_{ON} and R_{OFF} values. Therefore, an adaptation effect occurs in the system.

Future studies are planned to demonstrate the effectiveness of this simulation study, to test the proposed controller structure on a real system with a dead-time included system model, and to analyze the stability, sensitivity and frequency stability of the system.

REFERENCES

[1] C.-C. Tsai and C.-H. Lu, "Multivariable self-tuning temperature control for plastic injection molding process," *IEEE Trans. Ind. Appl.*, vol. 34, no. 2, pp. 310–318, Mar. 1998.

[2] H. S. Ahn, V. Bhambhani, and Y. Chen, "Fractional-order integral and derivative controller for temperature profile tracking," *Sadhana*, vol. 34, no. 5, pp. 833–850, 2009, doi: 10.1007/s12046-009-0049-2.

[3] U. Al-Saggaf, I. Mehedi, M. Bettayeb, and R. Mansouri, "Fractional-order controller design for a heat flow process," *Proc. Inst. Mech. Eng. I, J. Syst. Control Eng.*, vol. 230, no. 7, pp. 680–691, 2016, doi: 10.1177/0959651816649917.

[4] S. Khadraoui and H. Nounou, "A nonparametric approach to design fixed-order controllers for systems with constrained input," *Int. J. Control, Autom. Syst.*, vol. 16, no. 6, pp. 2870–2877, Dec. 2018, doi: 10.1007/s12555-017-0541-0.

[5] M. A. H. Pérez, B. del Muro Cuéllar, M. V. Villa, D. F. N. Rodríguez, R. A. G. Moctezuma, and P. J. G. Ramírez, "An improvement on the PI controller for a class of high-order unstable delayed systems: Application to a thermal process," *Control Eng. Appl. Informat.*, vol. 20, no. 1, pp. 25–35, 2018.

[6] U. M. Nath, C. Dey, and R. K. Mudi, "Fuzzy tuned model based control for level and temperature processes," *Microsyst. Technol.*, vol. 25, no. 3, pp. 819–827, 2019, doi: 10.1007/s00542-019-04300-x.

[7] A. Alhejji and M. I. Mosaad, "Performance enhancement of grid-connected PV systems using adaptive reference PI controller," *Ain Shams Eng. J.*, vol. 12, no. 1, pp. 541–554, 2021.

[8] J. R. Padhi, M. K. Debnath, and S. K. Kar, "Self-tuning fuzzy-PI controller for load frequency control analysis with the integration of wind energy," *Energy Sour. A, Recovery, Utilization, Environ. Effects*, vol. 44, no. 1, pp. 613–631, 2022.

[9] A. M. Hussien, R. A. Turky, A. Alkuhayli, H. M. Hasanien, M. Tostado-Véliz, F. Jurado, and R. C. Bansal, "Coot bird algorithms-based tuning PI controller for optimal microgrid autonomous operation," *IEEE Access*, vol. 10, pp. 6442–6458, 2022.

[10] S. J. Alam and S. R. Arya, "Volterra LMS/F based control algorithm for UPQC with multi-objective optimized PI controller gains," *IEEE J. Emerg. Sel. Topics Power Electron.*, Jan. 25, 2022, doi: 10.1109/JESTPE.2022.3146210.

[11] I. M. Horowitz, *Synthesis of Feedback Systems*. New York, NY, USA: University of Michigan Academic Press, 1963.

[12] J. Sánchez, A. Visioli, and S. A. Dormido, "A two-degree-of-freedom PI controller based on events," *J. Process Control*, vol. 21, no. 4, pp. 639–651, 2011.

[13] V. M. Alfaro and R. Vilanova, "Robust tuning and performance analysis of 2DoF PI controllers for integrating controlled processes," *Ind. Eng. Chem. Res.*, vol. 51, no. 40, pp. 13182–13194, 2012.

[14] Eke, M. Saka, H. Gozde, Y. Arya, and M. C. Taplamacioglu, "Heuristic optimization based dynamic weighted state feedback approach for 2DOF PI-controller in automatic voltage regulator," *Eng. Sci. Technol., Int. J.*, vol. 24, no. 4, pp. 899–910, 2021.

[15] D. Campos, O. Arrieta, R. Vilanova, and J. D. Rojas, "Robust tuning for 2DoF fractional-order PI controllers based on model reference approach," in *Proc. Int. Conf. Inf. Technol. Syst.*, San Carlos, Costa Rica, 2022, pp. 687–696.

[16] R. Guras, R. Strambersky, and M. Mahdal, "The PID and 2DOF control of the integral system-influence of the 2DOF parameters and practical implementation," *Meas. Control*, vol. 2022, Apr. 2022, Art. no. 00202940221076961.

[17] L. O. Chua, "Memristor-the missing circuit element," *IEEE Trans. Circuit Theory*, vol. CT-18, no. 5, pp. 507–519, Sep. 1971.

[18] D. B. Strukov, G. S. Snider, D. R. Stewart, and R. S. Williams, ''The missing memristor found,'' *Nature*, vol. 453, no. 7191, pp. 80–83, 2008.

[19] Z. Biolek, D. Biolek, and V. Biolkova, ''SPICE model of memristor with nonlinear dopant drift,'' *Radioengineering*, vol. 18, no. 2, pp. 1–15, 2009.

[20] A. Yeşil, Y. Babacan, and F. Kaçar, ''A new DDCC based memristor emulator circuit and its applications,'' *Microelectron. J.*, vol. 45, no. 3, pp. 282–287, 2014.

[21] Y. Babacan, A. Yesil, and F. Kacar, ''Memristor emulator with tunable characteristic and its experimental results,'' *AEU-Int. J. Electron. Commun.*, vol. 81, pp. 99–104, Nov. 2017.

[22] N. Raj, R. K. Ranjan, and F. Khateb, ''Flux-controlled memristor emulator and its experimental results,'' *IEEE Trans. Very Large Scale Integr. (VLSI) Syst.*, vol. 28, no. 4, pp. 1050–1061, Jan. 2020.

[23] S. S. Prasad, P. Kumar, and R. K. Ranjan, ''Resistorless memristor emulator using CFTA and its experimental verification,'' *IEEE Access*, vol. 9, pp. 64065–64075, 2021.

[24] Y. Babacan, A. Yesil, O. F. Tozlu, and F. Kacar, ''Investigation of STDP mechanisms for memristor circuits,'' *AEU-Int. J. Electron. Commun.*, vol. 151, Jul. 2022, Art. no. 154230.

[25] S. Zhu, L. Wang, and S. Duan, ''Memristor-based neural network PID controller for buck converter,'' in *Proc. IEEE 6th Int. Conf. Intell. Control Inf. Process. (ICICIP)*, Guizhou, China, Jun. 2015, pp. 36–41.

[26] C. Sánchez-López, F. E. Morales-López, and M. A. Carrasco-Aguilar, ''High-level simulation of a PID controller based on memristor,'' in *Proc. 14th IEEE Int. New Circuits Syst. Conf.*, Jun. 2016, pp. 1–4.

[27] Y. Lu, Q. Liang, and X. Huang, ''Parameters self-tuning PID controller circuit with memristors,'' *Int. J. Circuit Theory Appl.*, vol. 46, no. 1, pp. 138–154, 2018.

[28] K. Orman, ''Temperature profile tracking control with memristor based PI controller in the heat flow system,'' *Int. J. Modern Res. Eng. Technol.*, vol. 4, no. 12, pp. 12–15, 2019.

[29] C. Sánchez-López, V. H. Carbajal-Gómez, M. A. Carrasco-Aguilar, and F. E. Morales-López, ''PID controller design based on memductor,'' *AEU-Int. J. Electron. Commun.*, vol. 101, pp. 9–14, 2019.

[30] K. Orman, ''Memristor based PD controller design and application on a ball and beam control system,'' in *Proc. Int. Conf. Eng. Technol.*, Konya, Turkey, Nov. 2020, pp. 143–146.

[31] K. Orman, ''Design of a memristor-based chattering free sliding mode controller and speed control of the BLDC motor,'' *Tehnički Vjesnik*, vol. 28, no. 3, pp. 754–762, 2021.

[32] S. S. Biswal, D. R. Swain, and P. K. Rout, ''Design and analysis of memductor based PID controller for AVR,'' in *Innovation in Electrical Power Engineering, Communication, and Computing Technology*. Singapore: Springer, 2022, pp. 513–526.

[33] T. A. Wey and W. D. Jemison, ''Variable gain amplifier circuit using titanium dioxide memristors,'' *IET Circuits, Devices Systems*, vol. 5, no. 1, pp. 59–65, 2011.

[34] T. A. Wey and W. D. Jemison, ''An automatic gain control circuit with TiO_2 memristor variable gain amplifier,'' in *Proc. 8th IEEE Int. NEWCAS Conf.*, Montreal, QC, Canada, Jan. 2010, pp. 49–52, doi: 10.1109/NEWCAS.2010.5603719.

[35] T. A. Wey and W. D. Jemison, ''An automatic gain control circuit with TiO2 memristor variable gain amplifier,'' *Analog Integr. Circuits Signal Process.* vol. 73, no. 3, pp. 663–672, 2012, doi: 10.1007/s10470-012-9860-5.

[36] *Heat Flow Experiment Setup Courseware*. Accessed: 2014. [Online]. Available: http://www.www.quanser.com

[37] H. Huang, W. He, J. Wang, L. Zhang, and Q. Fu, ''An all servo-driven bird-like flapping-wing aerial robot capable of autonomous flight,'' *IEEE/ASME Trans. Mechatronics*, early access, Jun. 24, 2022, doi: 10.1109/TMECH.2022.3182418.

[38] Z. Han, Z. Liu, W. Kang, and W. He, ''Boundary feedback control of a nonhomogeneous wind turbine tower with exogenous disturbances,'' *IEEE Trans. Autom. Control*, vol. 67, no. 4, pp. 1952–1959, Apr. 2021, doi: 10.1109/TAC.2021.3071021.

[39] X. Wang, Y. Zhao, and Y. Liao, ''Dynamic performance analysis of PID controller with one memristor,'' in *Proc. IEEE Int. Conf. Inf. Sci. Technol.*, Nanjing, China, Mar. 2011, pp. 1234–1237.

[40] M. Viteckova and A. Vitecek, ''2DOF PI and PID controllers tuning,'' *IFAC Proc. Volumes*, vol. 43, no. 2, pp. 343–348, 2010.

KAMIL ORMAN received the B.Sc. degree in electrical and electronics engineering from Selcuk University, in 1996, and the M.Sc. and Ph.D. degrees in electrical and electronics engineering from Atatürk University, in 2008 and 2018, respectively. He is currently working as an Assistant Professor with the Computer Engineering Department, Erzincan Binali Yıldırım University. His main research interests include control systems, nonlinear control, algorithms, robotic systems, and unmanned vehicles.